

Peripheral three-body coupling model for knockout reactions

Arun K. Jain

Nuclear Physics Division, Bhabha Atomic Research Centre, Bombay 400 085, India

(Received 22 January 1991)

A new symmetric three-body coupling model has been developed for the description of the final state of knockout reactions. This model provides an exact description of the three-body final state when either one or both of the two distorting optical potentials vanish. Such a model gives a good description of the situation present in the knockout reactions in the extreme peripheral region, where at least one of the distorting optical potentials is ineffective. Comparison between the predictions of this model and the conventional kinematic coupling model for the 140 MeV ${}^2\text{H}(\alpha, \alpha'p)n$ reaction and the 90 MeV ${}^{16}\text{O}(\alpha, 2\alpha){}^{12}\text{C}$ reaction are illustrative of the conclusions which could be drawn from cluster knockout reaction analyses.

PACS number(s): 24.50.+g, 24.10.Eq

I. INTRODUCTION

In the past two decades increasing evidence has been gathered to show that the conventional distorted-wave impulse approximation (DWIA) used in conjunction with other associated approximations fails badly in reproducing the experimental data when the distortion effects are large [1–7]. Since most of the inputs to these calculations are very reliable, this failure in reproducing the data indicates the breakdown of some of the approximations made in the analyses [7]. In one of the papers published earlier [8] it has been shown that the approximation involved in replacing the three-body coupling term in the distorted-wave treatment of the three-body final state by its plane-wave contribution makes large changes in the knockout cross sections. This difference is seen to be large when the absorption in the optical potentials is small and the recoiling nucleus is light. The nonlocal three-body coupling term when expressed as local contributions to the optical potentials is seen [9] to depend strongly on the angular momentum, l , and its azimuthal projection, m . Furthermore, these effective decoupling potentials are strongly oscillating with no apparent predictability [9] in the position and strength of the kinks. Normally, for the cluster knockout reactions involving nuclear projectiles, the distortions introduced by optical potentials are large. For example, in the case of the ${}^{16}\text{O}(\alpha, 2\alpha){}^{12}\text{C}_{\text{g.s.}}$ reaction around 100 MeV the optical distortions reduce the cross sections by about three orders of magnitude [7]. Moreover, in these reactions the distortions cut down contributions from the nuclear interior to such an extent that the calculated energy sharing distribution is much sharper than that observed in the experiments. It appears therefore that the explanation of these anomalies lies in the improper treatment of the three-body final state. The theoretical treatment of the three-body final state, however, has not attracted much attention during the last two decades. The development of the diproton model (DPM) [10], the kinematic coupling approximation (KCA) [11,12], and the potential coupling model (PCM) [13] had taken place back in the late sixties. The inadequacy of the diproton model was

realized early [14] when it was pointed out that the neglect of the curvature and higher-order terms in the expansion of proton optical potentials around the diproton center of mass causes large asymmetries in the angular distributions due to an overestimation of distortions at large scattering angles. For the kinematic coupling approximation it was shown that for an exactly solvable test case [8] there exist differences of up to an order of magnitude in cross sections in addition to large variations in the shape of the energy sharing distribution. In the potential coupling approximation, however, a spurious asymmetry is introduced in the very beginning, which is clearly evident in an otherwise symmetric case.

In the present paper a new symmetric three-body equation has been described, for the three-body final state of knockout reactions, which overcomes many of the objections raised for the earlier three-body models. In this model, which is to be described in the next section, an exact solution of the three-body final state of knockout reaction is obtained (the reaction is being described in terms of the impulse approximation [11]) when either one or both of the distorting optical potentials vanish. The model may be called the peripheral three-body coupling model (PTBCM) because, with the normal kinematic conditions, a knockout reaction is localized in the nuclear peripheral region [7,13,15], where the influence of at least one of the optical potentials becomes small as the impact parameter is large in at least one of the two relative motions of the three-body system (see Fig. 1). The PTBCM will be seen to be applicable for the symmetric [reactions such as $(p, 2p)$, $(\alpha, 2\alpha)$, $(d, 2d)$, etc.] as well as the nonsymmetric [reactions such as $(e, e'p)$, $(p, p\alpha)$, $(d, d\alpha)$, $(\alpha, \alpha p)$, etc.] final state of the system. Section II outlines the formalism of PTBCM and general results and discussion using this formalism for ${}^2\text{H}(\alpha, \alpha'p)n$ and ${}^{16}\text{O}(\alpha, 2\alpha){}^{12}\text{C}$ reactions are presented in Sec. III. General conclusions for the DWIA analyses of knockout reactions following the PTBCM constitute Sec. IV.

II. PTBCM FORMALISM

The three-body final-state Hamiltonian \mathcal{H}_f for a knockout reaction $A(a, ab)B$, which is usually described

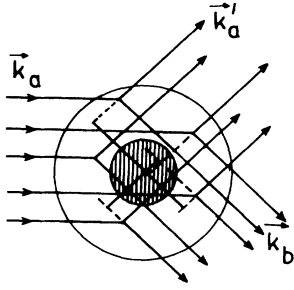


FIG. 1. Schematic trajectories for knockout reactions in the peripheral region. The central shaded region represents the strong absorption zone in the target nucleus.

in terms of impulse approximation, is

$$\mathcal{H}_f = H_a + H_b + H_B + T_a + T_b + T_B + V_{aB}(r_{aB}) + V_{bB}(r_{bB}). \quad (1)$$

Here H_x and T_x are, respectively, the internal Hamiltonian and kinetic energy operators for particle x and $V_{xy}(r_{xy})$ is the distorting optical potential for the x - y relative motion. The impulse approximation takes care of the knockout interaction V_{ab} and is thus not included as part of this \mathcal{H}_f . The interaction V_{ab} forms part of the factorization approximation. In this approximation the matrix element of this interaction between the initial and final a - b scattering states is separated from the rest of the matrix element [11,16], which is subsequently expressed in terms of the on-shell free a - b scattering cross section. Reexpressing \mathcal{H}_f in Eq. (1) in terms of relative coordinates \mathbf{r}_{aB} and \mathbf{r}_{bB} (see Fig. 2) and suppressing the center of mass and intrinsic Hamiltonians, we have

$$\mathcal{H}_f = \dots - \frac{\hbar^2}{2\mu_{aB}} \nabla_{aB}^2 - \frac{\hbar^2}{2\mu_{bB}} \nabla_{bB}^2 - \frac{\hbar^2}{m_B} \nabla_{aB} \cdot \nabla_{bB} + V_{aB}(r_{aB}) + V_{bB}(r_{bB}). \quad (2)$$

In the conventional DWIA calculations the three-body coupling term $-(\hbar^2/m_B) \nabla_{aB} \cdot \nabla_{bB}$ is approximated by its asymptotic plane-wave limit [7,13], $(\hbar^2/m_B) \mathbf{k}_{aB} \cdot \mathbf{k}_{bB}$. This so-called kinematic coupling approximation [8] (KCA) includes only the kinematic part of the coupling, while the dynamic component in it, arising due to the distorting optical potentials, V_{aB} and V_{bB} , is neglected here. The KCA formalism leads to a three-body final-state wave function which is factorizable into two two-body scattering-state wave functions with their respective boundary conditions [11,12]:

$$\Psi_{f_1}^{(-)}(\text{KCA})(\mathbf{r}_{aB}, \mathbf{r}_{bB}) = \chi_1^{(-)}(\mathbf{k}_{aB}, \mathbf{r}_{aB}) \chi_2^{(-)}(\mathbf{k}_{bB}, \mathbf{r}_{bB}), \quad (3)$$

where

$$\Psi_{f_1}^{(-)}(\text{PCM})(\mathbf{r}_{aA}, \mathbf{r}_{bB}) = \exp(i\mathbf{k}_{aB} \cdot \mathbf{r}_{aB}) \exp \left[-i \frac{m_b}{(m_b + m_B)} \mathbf{k}_{aB} \cdot \mathbf{r}_{bB} \right] \chi_3^{(-)}(\mathbf{k}'_{bB}, \mathbf{r}_{bB}). \quad (9)$$

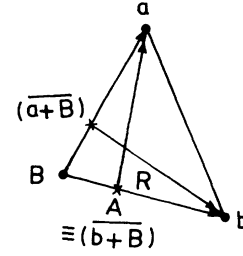


FIG. 2. The two combinations of relative coordinates $(\mathbf{r}_{aA}, \mathbf{r}_{bB})$ and $(\mathbf{r}_{b(a+B)}, \mathbf{r}_{aB})$ used in the formulation of the PTBCM.

$$\mathbf{k}_{aB} = \mathbf{k}'_a - \frac{m_a}{(m_a + m_b + m_B)} \mathbf{k}_a, \quad (4)$$

$$\mathbf{k}_{bB} = \mathbf{k}_b - \frac{m_b}{(m_a + m_b + m_B)} \mathbf{k}_a,$$

where \mathbf{k}_a is the incident wave vector of projectile a and \mathbf{k}'_a , \mathbf{k}_b , and \mathbf{k}_B are the final-state wave vectors of a , b , and B , respectively, in the laboratory frame.

Now consider another set of relative coordinates \mathbf{r}_{aA} and \mathbf{r}_{bB} (see Fig. 2). The \mathcal{H}_f expressed in terms of operators conjugate to these relative coordinates [11,13] reads as

$$\mathcal{H}_f = \dots - \frac{\hbar^2}{2\mu_{aA}} \nabla_{aA}^2 - \frac{\hbar^2}{2\mu_{bB}} \nabla_{bB}^2 + V_{aB}(r_{aB}) + V_{bB}(r_{bB}). \quad (5)$$

In this representation the three-body coupling manifests itself through the interaction $V_{aB}(r_{aB})$, which is function of r_{aB} and not of r_{aA} (the coordinate corresponding to \mathbf{r}_{aA} appears in the kinetic energy operator) [11]. When $V_{aB}(r_{aB})$ vanishes, one obtains the exact solution of Eq. (5) in this so-called potential coupling formalism as [8]

$$\Psi_{f_1}^{(-)}(\text{PCM})(\mathbf{r}_{aA}, \mathbf{r}_{bB}) = \exp(i\mathbf{k}'_{aA} \cdot \mathbf{r}_{aA}) \chi_3^{(-)}(\mathbf{k}'_{bB}, \mathbf{r}_{bB}), \quad (6)$$

where

$$\mathbf{k}'_{aA} = \mathbf{k}'_a - \frac{m_a}{(m_a + m_b + m_B)} \mathbf{k}_a, \quad (7)$$

$$\mathbf{k}'_{bB} = \frac{(m_B \mathbf{k}_b - m_b \mathbf{k}_B)}{(m_b + m_B)}.$$

It is to be inferred from Eqs. (4) and (7) that $\mathbf{k}'_{aA} = \mathbf{k}_{aB}$ and from Fig. 2 that

$$\mathbf{r}_{aA} = \mathbf{r}_{aB} - \frac{m_b}{(m_b + m_B)} \mathbf{r}_{bB}. \quad (8)$$

With this the wave function $\Psi_{f_1}^{(-)}(\text{PCM})(\mathbf{r}_{aA}, \mathbf{r}_{bB})$ of Eq. (6) can be written exactly as

From here one gets the \mathbf{r}_{bB} dependent factor of the final-state wave function (when $V_{aB}=0$) as

$$\Psi_{bB}^{(-)}(\mathbf{r}_{bB}) = \exp \left[-i \frac{m_b}{(m_b + m_B)} \mathbf{k}_{aB} \cdot \mathbf{r}_{bB} \right] \chi_3^{(-)}(\mathbf{k}'_{bB}, \mathbf{r}_{bB}) . \quad (10)$$

This is the exact wave function of the b - B relative motion when the a - B interaction potential, V_{aB} in Eq. (2), vanishes. In the KCA the corresponding b - B relative motion wave function is, however, given by $\chi_2^{(-)}(\mathbf{k}_{bB}, \mathbf{r}_{bB})$ of Eq. (3). The wave function $\Psi_{bB}^{(-)}(\mathbf{r}_{bB})$ of Eq. (10) has been found [9] to be the solution of a Schrödinger equation with local potentials which have sharp kinks and which vary strongly with orbital angular momentum, l , as well as with its azimuthal projection, m . The wave function $\Psi_{bB}^{(-)}(\mathbf{r}_{bB})$ has the required feature that it represents the b - B solution of the three-body final state when the potential between a and B vanishes [8].

Consider now a situation where, instead of the interaction between a and B , the interaction between b and B vanishes. The eigenfunction of the final-state Hamiltonian for this situation can be obtained in terms of the relative coordinates \mathbf{r}_{aB} and $\mathbf{r}_{b(a+B)}$ (see Fig. 2) in the same

manner as outlined above for the case where V_{aB} vanishes. The solution $\Psi_{f_2(\text{PCM})}^{(-)}$ with the required boundary conditions is [8]

$$\Psi_{f_2(\text{PCM})}^{(-)}[\mathbf{r}_{aB}, \mathbf{r}_{b(a+B)}] = \exp[i\mathbf{k}_{b(a+B)} \cdot \mathbf{r}_{b(a+B)}] \chi_4^{(-)}(\mathbf{k}'_{aB}, \mathbf{r}_{aB}) , \quad (11)$$

where

$$\mathbf{k}'_{b(a+B)} = \mathbf{k}_b - \frac{m_b}{(m_a + m_b + m_B)} \mathbf{k}_a , \quad (12)$$

$$\mathbf{k}'_{aB} = \frac{(m_B \mathbf{k}'_a - m_a \mathbf{k}_B)}{(m_a + m_B)} .$$

Now from Fig. 2 it can be seen that

$$\mathbf{r}_{b(a+B)} = \mathbf{r}_{bB} - \frac{m_a}{(m_a + m_B)} \mathbf{r}_{aB} , \quad (13)$$

so that the wave function

$$\Psi_{f_2(\text{PCM})}^{(-)}[\mathbf{r}_{aB}, \mathbf{r}_{b(a+B)}]$$

of Eq. (11) can be written exactly as

$$\Psi_{f_2(\text{PCM})}^{(-)}[\mathbf{r}_{aB}, \mathbf{r}_{b(a+B)}] = \exp(i\mathbf{k}_{bB} \cdot \mathbf{r}_{bB}) \exp[-i \frac{m_a}{(m_a + m_B)} \mathbf{k}_{bB} \cdot \mathbf{r}_{aB}] \chi_4^{(-)}(\mathbf{k}'_{aB}, \mathbf{r}_{aB}) . \quad (14)$$

From here the \mathbf{r}_{aB} -dependent factor of the final-state wave function (when $V_{bB}=0$) becomes

$$\Psi_{aB}^{(-)}(\mathbf{r}_{aB}) = \exp \left[-i \frac{m_a}{(m_a + m_B)} \mathbf{k}_{bB} \cdot \mathbf{r}_{aB} \right] \chi_4^{(-)}(\mathbf{k}'_{aB}, \mathbf{r}_{aB}) . \quad (15)$$

This $\Psi_{aB}^{(-)}(\mathbf{r}_{aB})$ represents the exact a - B relative motion of the three-body final state when the b - B interaction, V_{bB} , vanishes. In the KCA, however, the corresponding wave function is represented by $\chi_1^{(-)}(\mathbf{k}_{aB}, \mathbf{r}_{aB})$.

It is obvious that $\Psi_{aB}^{(-)}(\mathbf{r}_{aB})$ and $\Psi_{bB}^{(-)}(\mathbf{r}_{aB})$ [of Eqs. (15) and (10)] are the solutions of

$$\left[-\frac{\hbar^2}{2\mu_{aB}} \nabla_{aB}^2 - \frac{\hbar^2}{2\mu_{bB}} \nabla_{bB}^2 - i \frac{\hbar^2}{m_B} \nabla_{aB} \cdot \mathbf{k}_{bB} - i \frac{\hbar^2}{m_B} \nabla_{bB} \cdot \mathbf{k}_{aB} - \frac{\hbar^2}{m_B} \mathbf{k}_{aB} \cdot \mathbf{k}_{bB} + V_{aB}(r_{aB}) + V_{bB}(r_{bB}) - \left[E_{aB} + E_{bB} + \frac{\hbar^2}{m_B} \mathbf{k}_{aB} \cdot \mathbf{k}_{bB} \right] \right] \Psi_{aB}^{(-)}(\mathbf{r}_{aB}) \Psi_{bB}^{(-)}(\mathbf{r}_{bB}) = 0 . \quad (18)$$

It is to be remarked here that this equation corresponds to a three-body Hamiltonian of the type of Eq. (2) with the difference that the coupling term [$T_{\text{coup}} = -(\hbar^2/m_B) \nabla_{aB} \cdot \nabla_{bB}$] is replaced by the following

$$\left[-\frac{\hbar^2}{2\mu_{aB}} \nabla_{aB}^2 - i \frac{\hbar^2}{m_B} \nabla_{aB} \cdot \mathbf{k}_{bB} + V_{aB}(r_{aB}) - \left[E_{aB} + \frac{\hbar^2}{m_B} \mathbf{k}_{aB} \cdot \mathbf{k}_{bB} \right] \right] \Psi_{aB}^{(-)}(\mathbf{r}_{aB}) = 0 \quad (16)$$

and

$$\left[-\frac{\hbar^2}{2\mu_{bB}} \nabla_{bB}^2 - i \frac{\hbar^2}{m_B} \nabla_{bB} \cdot \mathbf{k}_{aB} + V_{bB}(r_{bB}) - \left[E_{bB} + \frac{\hbar^2}{m_B} \mathbf{k}_{aB} \cdot \mathbf{k}_{bB} \right] \right] \Psi_{bB}^{(-)}(\mathbf{r}_{bB}) = 0 , \quad (17)$$

respectively. Here $E_{xB} = (\hbar^2/2\mu_{xB}) k_{xB}^2$, μ_{xB} is the x - B reduced mass, and \mathbf{k}_{xB} are the wave vectors given in Eq. (4). The product $\Psi_{aB}^{(-)}(\mathbf{r}_{aB}) \Psi_{bB}^{(-)}(\mathbf{r}_{bB})$ represents the solution of the following equation:

term:

$$T_{\text{coup}} = -i \frac{\hbar^2}{m_B} \nabla_{aB} \cdot \mathbf{k}_{bB} - i \frac{\hbar^2}{m_B} \mathbf{k}_{aB} \cdot \nabla_{bB} - \frac{\hbar^2}{m_B} \mathbf{k}_{aB} \cdot \mathbf{k}_{bB} . \quad (19)$$

With this replacement the coupling between the relative coordinates \mathbf{r}_{aB} and \mathbf{r}_{bB} in the final-state wave function is eliminated as the corresponding solution is the solution of Eq. (18), i.e., the product $\Psi_{aB}^{(-)}(\mathbf{r}_{aB})\Psi_{bB}^{(-)}(\mathbf{r}_{bB})$.

It is not difficult to verify that, when at least one of the distorting optical potentials vanishes in the \mathcal{H}_f of Eq. (2), the approximate coupling term of Eq. (19) has the same effect as the exact coupling term.

Although the solution $\Psi_{aB}^{(-)}(\mathbf{r}_{aB})\Psi_{bB}^{(-)}(\mathbf{r}_{bB})$ of Eq. (18) is separable as functions of \mathbf{r}_{aB} and \mathbf{r}_{bB} , it is seen that it involves the product of two plane waves and two distorted waves. Even with the presence of $\delta(\mathbf{r}_{ab})$, arising from the factorization in the DWIA matrix element [7,11,16,17], this can only be reduced to a product of three functions, one plane wave and two distorted waves. This PTBCM final state along with the initial-state wave function is practically unmanageable when using partial-wave expansions and subsequent angular momentum couplings [7,11,17]. Therefore, all the functions are calculated explicitly as functions of the corresponding polar coordinates, (r, θ, Φ) . The DWIA matrix element [11,17] can then be evaluated by using numerical quadrature techniques [18].

III. DWIA RESULTS

A. ${}^2\text{H}(\alpha, \alpha p)n$ reaction at 140 MeV

In order to examine the influence of the three-body coupling in the final state, the reaction ${}^2\text{H}(\alpha, \alpha p)n$ at 140 MeV [19] has been analyzed first. The small mass of the residual neutron is expected to enhance the three-body coupling term for this reaction [11]. Besides, the short-range nature of the p - n interaction, treated as a distortion in this calculation, makes one expect the approximations of the PTBCM to be valid in the region most important for this reaction. However, the distortion effects are not expected to be very pronounced here because the distorting optical potentials are not large. This is reflected in the comparatively large ratio of about 0.3 between the results of conventional DWIA calculations and the corresponding plane-wave results for this reaction [11].

The PTBCM, KCA, and PW results (normalized to the experimental data at the peak position) are compared with the observed energy sharing distribution in Fig. 3. It is to be remarked here that, in comparison with the KCA calculation, the overall shape is better reproduced by the PTBCM calculation. The plane-wave predictions are, of course, seen to deviate very much from the observed shape of the spectrum.

In Table I the magnitudes of the cross sections are compared. It is seen that the PW cross section is about a factor of 6.5 too large, while the KCA and the PTBCM predictions are larger by factors of about 2.8 and 2.2, respectively. It is to be kept in mind that there is an additional factor of about 2 between our calculated cross sections and that of Nadasen *et al.* [19] which appears to arise from the difference in the normalization of the bound deuteron wave function. In the present work we have used a Hulthén wave function with parameters from Ref. [20]. Based on these comparisons of the shape and

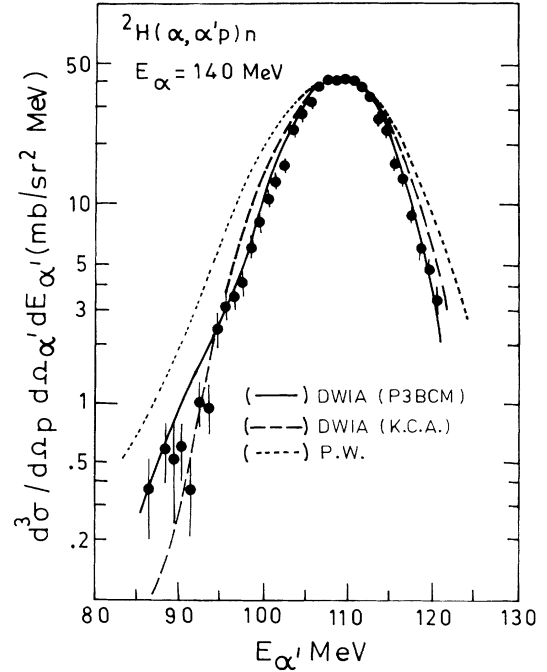


FIG. 3. Comparison of 140 MeV ${}^2\text{H}(\alpha, \alpha' p)n$ reaction [19] data and PTBCM calculations (—), KCA calculations (---), and plane-wave (PW) calculations (····). The calculated results are normalized at the peak position of $E_{\alpha'} = 108$ MeV.

magnitude of the ${}^2\text{H}(\alpha, \alpha p)n$ reaction at 140 MeV, it can be concluded that in the DWIA formalism the PTBCM description of the three-body final state provides a better method than the conventional KCA description.

B. ${}^{16}\text{C}(\alpha, 2\alpha){}^{12}\text{C}_{g.s.}$ reaction at 90 MeV

Looking at Fig. 1 one gets the feeling that, as long as one of the two emitted particles passes through the strongly absorbing shaded region, the contributions from the peripheral regions will also be suppressed. In accord with this, our calculations show (see Fig. 4) that the use of commonly employed strongly absorbing optical potentials for α particles [7,21] gives rise to no appreciable difference between the KCA and PTBCM results for the 90 MeV ${}^{16}\text{O}(\alpha, 2\alpha){}^{12}\text{C}_{g.s.}$ reaction [22]. This behavior is contrary to what is seen in Fig. 3 for the ${}^2\text{H}(\alpha, \alpha p)n$ reaction where the distortions are small and significant changes are seen in the predictions of the KCA and PTBCM prescriptions.

In order to investigate the influence of the three-body coupling in the final state of the 90 MeV ${}^{16}\text{O}(\alpha, 2\alpha){}^{12}\text{C}$ reaction calculations of the KCA and PTBCM prescrip-

TABLE I. Comparison of peak cross sections for 140 MeV ${}^2\text{H}(\alpha, \alpha p)n$ reaction using various formalisms (experimental value $\cong 42$ mb/sr² MeV).

Formalism	PW	KCA	PTBCM
Peak cross section (mb/sr ² MeV)	320.5	115.0	89.0

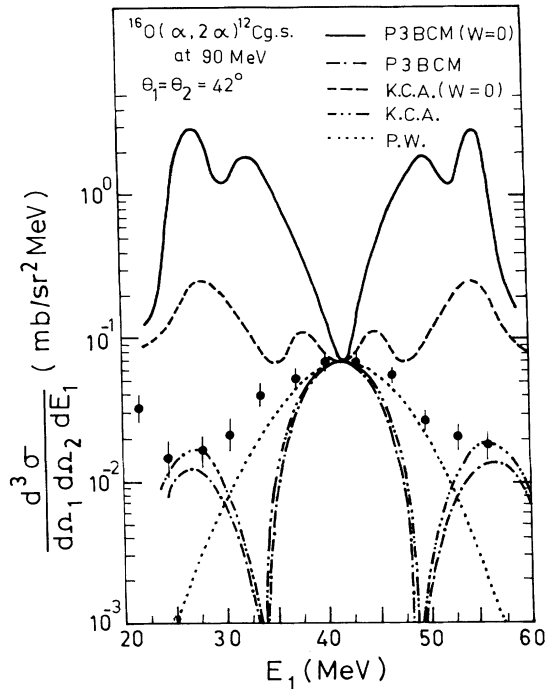


FIG. 4. Comparison of 90 MeV $^{16}\text{O}(\alpha, 2\alpha)^{12}\text{C}_{g.s.}$ reaction data and PTBCM calculations, with all imaginary potentials zero ($W=0$) (—), with full optical potentials (— · — · —); KCA calculations with all imaginary potentials zero ($W=0$) (---), with full optical potentials (--- · --- · ---); and plane-wave (PW) calculations (····).

tions are compared when the imaginary parts of all the optical potentials are taken to be zero. Although this choice was made *ad hoc*, it provides us with an insight into the influence of three-body coupling for the knockout reactions in the DWIA framework. With this choice it is seen in Fig. 4 that the energy sharing spectrum, which should have peaked at recoil momentum zero,

$$q=0 (E_{\alpha_1}=E_{\alpha_2}\cong 41.42 \text{ MeV}),$$

has very pronounced minima for both PTBCM and KCA calculations. Moreover, the PTBCM spectrum (normalized to the experimental peak position at $E_{\alpha}=41.42$ MeV) varies more sharply than the KCA spectrum. In fact, the calculated shapes of the spectra look more like $l\neq 0$ distributions, which normally have dips at $q\cong 0$. Besides, at $q=0$ the absolute cross sections (in $\text{mb}/\text{sr}^2\text{MeV}$) produced by the KCA and PTBCM are 0.076 and 0.00156, respectively, while the experimental value is ~ 0.07 . Calculations with the commonly employed optical potentials, however, give cross-section values of 0.006 and 0.0066 for KCA and PTBCM, respectively. These are much lower than the observations. Besides this the DWIA prediction, in both the prescriptions, of the shape of the spectrum is also much too sharp. In comparison to these frustrating results, the plane-wave (PW) results are in fact much closer to the observations: at least the shape of the spectrum is well reproduced, although the absolute cross section is pre-

dicted to be more than two orders of magnitude too large.

Although it is difficult to arrive at any general conclusions from these analyses, one gets the feeling that a scaling down of the effects of the complete distorting potentials can bridge the large gap between the DWIA calculations and the experimental data. A justification and understanding of such a scaling down of the optical potentials by the decoupling of the three-body system into two two-body systems are yet to be obtained. An indication to the effect that the decoupling of relative coordinates in a coupled three-body system leads to a new set of effective potentials (called effective decoupling potentials) has already been found in the special case when one of the optical potentials vanishes. In that case the effective decoupling potentials have been found to depend strongly on the partial-wave angular momentum and on its component in the z direction. These effective decoupling potentials were also shown to have sharp kinks and large variations as functions of the separation distance. For a realistic case the influence of the three-body coupling on the decoupling potentials can only be expected to be much more dramatic.

IV. CONCLUSIONS

A new description, called the peripheral three-body coupling model (PTBCM), has been reported, which exactly takes care of the three-body dynamic coupling term in the final state of knockout reactions when one or both of the outgoing particles are assumed not to interact with the residual nucleus. Similarly to the kinematic coupling model (KCA), the PTBCM is symmetric in the description of the two relative motions in the final state. The approximation in the PTBCM is in the treatment of the three-body dynamic coupling when the trajectories of both outgoing particles are strongly altered by their interaction with the residual nucleus. This model is expected to provide a better understanding of $(e, e'x)$ reactions, where use of the KCA or the potential coupling model (PCM) encounters some difficulties [23]. The PTBCM prescription for the 140 MeV $^2\text{H}(\alpha, \alpha p)n$ reaction has been seen to describe the shape as well as the magnitude of the cross section better than the KCA prescription. For the description of the 90 MeV $^{16}\text{O}(\alpha, 2\alpha)^{12}\text{C}_{g.s.}$ reaction, however, both these prescriptions were found to be in gross disagreement with the experimental data, in shape as well as in magnitude. Large differences have been found in the predictions of the two prescriptions when the absorptive parts of the optical potentials were not incorporated into the calculations. With this prescription applied the shape agreement with experiment is worsened further, and the KCA absolute cross section at recoil momentum zero is almost 50 times larger than the PTBCM prediction of 0.00156 $\text{mb}/\text{sr}^2\text{MeV}$. This comparison therefore indicates that the absorptive part of the optical potential is not the only one responsible for the disagreement [24] between the theory and the experimental data for cluster knockout reactions. It indicates further than an agreement between the DWIA prediction and experiment can be achieved by some scaling

down of the optical potential as a whole [25]. An indication that a modification of the optical potentials used in the DWIA analyses is required has already been seen in the decoupling potentials for the three-body final state in the special case when one of the final-state optical potentials is assumed to vanish. One can only expect to find the influence of the three-body dynamic coupling on the

respective decoupling potentials to be enhanced for a realistic situation.

The author is grateful to Dr. N. Sarma for constructive criticism and encouragement for this work and to Dr. Amit Roy for computational support and helpful discussions.

-
- [1] C. W. Wang, N. S. Chant, P. G. Roos, A. Nadasen, and T. A. Carey, *Phys. Rev. C* **21**, 1705 (1980).
- [2] T. A. Carey, P. G. Roos, N. S. Chant, A. Nadasen, and H. L. Chan, *Phys. Rev. C* **29**, 1273 (1984).
- [3] P. G. Roos and N. S. Chant, in *Proceedings of the Second International Conference on Clustering Phenomena in Nuclei*, University of Maryland, 1975, edited by D. A. Goldberg, J. B. Marion, and S. J. Wallace (National Technical Information Service, Springfield, Virginia, 1975), p. 242.
- [4] N. S. Chant, P. G. Roos, and C. W. Wang, *Phys. Rev. C* **17**, 8 (1978).
- [5] C. Samanta, N. S. Chant, P. G. Roos, A. Nadasen, and A. A. Cowley, *Phys. Rev. C* **26**, 1379 (1982).
- [6] S. H. Yoo *et al.*, *Phys. Rev. Lett.* **63**, 738 (1989).
- [7] N. S. Chant and P. G. Roos, *Phys. Rev. C* **15**, 57 (1977).
- [8] A. K. Jain, *Phys. Rev. C* **42**, 368 (1990).
- [9] A. K. Jain, *Pramana J. Phys.* **37**, 281 (1991).
- [10] D. F. Jackson, *Nucl. Phys.* **A90**, 209 (1967).
- [11] D. F. Jackson and T. Berggren, *Nucl. Phys.* **62**, 355 (1965).
- [12] K. L. Lim and I. E. McCarthy, *Phys. Rev.* **113B**, 1006 (1964).
- [13] A. K. Jain, J. Y. Grossiord, M. Chevallier, P. Gaillard, A. Guichard, M. Gusakov, and J. R. Pizzi, *Nucl. Phys.* **A216**, 519 (1973).
- [14] B. K. Jain and D. F. Jackson, *Nucl. Phys.* **A99**, 113 (1967).
- [15] B. K. Jain, *Nucl. Phys.* **A129**, 145 (1969).
- [16] G. Jacob and Th. A. J. Maris, *Rev. Mod. Phys.* **38**, 121 (1966).
- [17] A. K. Jain, N. Sarma, and B. Banerjee, *Nucl. Phys.* **A142**, 330 (1970).
- [18] N. S. Chant, University of Maryland Cyclotron Laboratory Progress Report, 1977, p. 65.
- [19] A. Nadasen, T. A. Carey, P. G. Roos, N. S. Chant, C. W. Wang, and H. L. Chan, *Phys. Rev. C* **19**, 2099 (1979).
- [20] L. Hulthén and M. Sugawara, *Handbuch der Physik* **39**, 32 (1957); **39**, 74 (1957).
- [21] P. P. Singh, R. E. Malmin, M. High, and D. W. Devins, *Phys. Rev. Lett.* **23**, 1124 (1969).
- [22] J. D. Sherman, D. L. Hendrie, and M. S. Zisman, *Phys. Rev. C* **13**, 20 (1976).
- [23] L. B. J. M. Lanen, H. P. Blok, E. Jans, L. Lapikas, G. van der Steenhoven, and P. K. A. de Witt Huberts, *Phys. Rev. Lett.* **64**, 2250 (1990); C. Giusti and F. D. Picati, *Nucl. Phys.* **A473**, 717 (1987).
- [24] D. F. Geesaman *et al.*, *Phys. Rev. Lett.* **63**, 734 (1989).
- [25] A. K. Jain and N. Sarma, *Nucl. Phys.* **A321**, 429 (1979).